Functionalization of Graphene Nanoplatelets Using Sugar Azide for Graphene/Epoxy Nanocomposites

Saswata Bose[1], Lawrence T. Drzal [1*]

Dept of Chemical Engineering and Materials Science
Composite Materials and Structures Center
Michigan State University, MI-48823, USA

*** Corresponding Author**

E-mail: Drzal@egr.msu.edu (L.T.Drzal)

Tel: (517) 353-7759

Report Documentation Page

Form Approved
OMB No. 0704-0188

1. REPORT DATE	2. REPORT TYPE	3. DATES COVERED
20 JUN 2014	**Technical Report**	**09-02-2014 to 22-05-2014**

4. TITLE AND SUBTITLE
FICTIONALIZATION OF GRAPHENE NANOPLATELETS USING SUGAR AZIDE FOR GRAPHENE/EPOXY NANOCOMPOSITES

5a. CONTRACT NUMBER
W56HZV-13-C-0401

5b. GRANT NUMBER

5c. PROGRAM ELEMENT NUMBER

6. AUTHOR(S)
Saswata Bose; Lawrence Drzal

5d. PROJECT NUMBER

5e. TASK NUMBER

5f. WORK UNIT NUMBER

7. PERFORMING ORGANIZATION NAME(S) AND ADDRESS(ES)
Dept of Chemical Engineering and Materials Science,Composite Materials and Structures Center,2100 Engineering Building,East Lansing,Mi,48824-1226

8. PERFORMING ORGANIZATION REPORT NUMBER
; #24960

9. SPONSORING/MONITORING AGENCY NAME(S) AND ADDRESS(ES)
U.S. Army TARDEC, 6501 East Eleven Mile Rd, Warren, Mi, 48397-5000

10. SPONSOR/MONITOR'S ACRONYM(S)
TARDEC

11. SPONSOR/MONITOR'S REPORT NUMBER(S)
#24960

12. DISTRIBUTION/AVAILABILITY STATEMENT
Approved for public release; distribution unlimited

13. SUPPLEMENTARY NOTES
For JOURNAL OF CARBON LETTERS

14. ABSTRACT
We report a covalent functionalization of graphene nanoparticles (GnPs) employing 2,3,4-Tri-O-acetyl-β-D-xylopyranosyl azide followed by fabrication of an epoxy/functionalized graphene nanocomposite and its thermo-mechanical performance evaluation. Successful functionalization of GnP was confirmed via TGA and XPS study. Raman spectroscopy indicated that the functionalization was on the edge of graphene sheets as the basal plane was not perturbed as a result of the functionalization. Epoxy/functionalized GnP composite system produced an increase in the flexural modulus (~18%) and glass transition temperature (~10C) compared to an un-functionalized GnP based epoxy composite.

15. SUBJECT TERMS
Graphene nanoparticles, Sugar Azide, Nanocomposite, Spectroscopy, Thermo-mechanical property.

16. SECURITY CLASSIFICATION OF:			17. LIMITATION OF ABSTRACT	18. NUMBER OF PAGES	19a. NAME OF RESPONSIBLE PERSON
a. REPORT	b. ABSTRACT	c. THIS PAGE			
unclassified	**unclassified**	**unclassified**	**Public Release**	**22**	

Abstract

We report a covalent functionalization of graphene nanoparticles (GnPs) employing 2,3,4-Tri-O-acetyl-β-D-xylopyranosyl azide followed by fabrication of an epoxy/functionalized graphene nanocomposite and its thermo-mechanical performance evaluation. Successful functionalization of GnP was confirmed via TGA and XPS study. Raman spectroscopy indicated that the functionalization was on the edge of graphene sheets as the basal plane was not perturbed as a result of the functionalization. Epoxy/functionalized GnP composite system produced an increase in the flexural modulus (~18%) and glass transition temperature (~10^{O}C) compared to an un-functionalized GnP based epoxy composite.

Keywords: Graphene nanoparticles, Sugar Azide, Nanocomposite, Spectroscopy, Thermo-mechanical property.

1. Introduction

Graphene, a one atom thick, 2D lattice of sp^2-bonded carbon atoms [1-3], has received significant attention from researchers over the world owing to its excellent optical, mechanical and electrical properties [4-9]. Graphene sheets are held together by van dar Waals force of attraction. However the inherent tendency towards restacking limits their applications. Incorporation of polar groups such as carboxyl, hydroxyl via covalent/non-covalent functionalization approach might be a fruitful method to achieve stable dispersion of graphene sheets in a polymer. Stable aqueous or organic suspensions of graphene have been achieved via chemical modification and/or oxidation–reduction of graphite oxide [10-12]. However, functionalization of graphene via chemical oxidation-reduction method requires the involvement of strong and hazardous acids which in turn destroys sp^2 carbon network and changes the sp^2 hybridized graphene into a sp^3 network with significantly reduced properties. This report has investigated sugar azide for the edge-functionalization of graphene via covalent bond formation without disrupting the graphene structure. Sugars are very rich in hydroxyl groups and are therefore chosen as potential material for functionalization. The aim of our study is to create additional –OH group on the GnP in order to achieve a stable dispersion in polar organic solvent without disrupting the basal plane of graphene. The additional polar groups are also beneficial as

sites for covalent bond formation with an epoxy matrix and thus contribute towards the themo-mechanical property enhancement of epoxy/graphene nanocomposite.

2. Experimental Details

2.1. Materials

GnP (Size:15 µm, Thickness:5-7 nm, Surface area: 120-150 m^2/g) was supplied by XG Sciences, USA. 2,3,4-Tri-O-acetyl-β-D-xylopyranosyl azide, known as Sugar azide (SA) was purchased from Sigma Aldrich. Epoxy (Epon 828) was purchased from Miller Stephenson. Ethyl acetate (EtOAc), sodium methoxide (NaOMe) and Metaphenylene Diamine (MPDA) were purchased from Sigma Aldrich.

2.2. Functionalization of GnP using Sugar Azide

A weighed amount of GnP was mixed with 1,1,2,2-tetrachloroethane (TCE) and the mixture was ultrasonicated for 10 min. The solution was then purged with nitrogen and preheated to 150^oC. Subsequently, Sugar azide (SA) was dispersed in TCE and the solution was added drop-wise to the reaction mixture over a period of 20–30 min. The temperature was maintained at 150^oC for 1 hour, after which the product was cooled to room temperature under flowing nitrogen . EtOAc was added into the cooled reaction mixture. The crude product will filtered on 0.22µm teflon membrane and washed copiously with EtOAc and Methanol (MeOH). The residue left on the filter paper was dried under vacuum at 50^OC overnight and this product was labelled as azide-functionalized GnP (SAMG-I). SAMG-I was mixed with ethanol (EtOH) followed by addition of NaOMe (30%) in MeOH. The reaction mixture was stirred under nitrogen for 24 hours at room temperature and then was slowly transferred into distilled water drop by drop. The basic mixture was then neutralized with a few drops of HCl (37%). The deacylated product was then filtered on 0.22µm teflon membrane and repeatedly washed with distilled water and EtOAc. Finally, the (SAMG) was dried at 50 °C under vacuum overnight.

2.2. Fabrication of Epoxy/GnP composite

Epoxy was mixed with SAMG using a Flack-tek speed mixer for 2 mins at 2500 rpm followed by ultrasonication for 30 mins at 60 watts. The solution was degassed in vacuum for 5 mins. MPDA was added to the mixture and again mixed using a Flack-tek speed mixer for 2 mins at

2000 rpm. The entire mixture was degassed for 5 mins at 70^{O}C. The solution was poured into a silicone mold to make coupons. The mixture was cured at 75^{O}C for 2 hours and at 125^{O}C for another 2 hours. The coupons were polished prior to testing.

3. Measurements

Raman spectra were recorded in the range of 500 to 3500 cm^{-1} in a LabRAM ARAMIS confocal Raman Microscope using a He-Cd laser beam with a wave length of 532 nm. X-ray photo electron spectroscopy (XPS) was performed with a Perkin Elmer Phi 5600 ESCA (Kratos Analytical Ltd, UK), using an unmonochromatized Mg-Kα X-ray source at a take-off angle of 45^{o}. Dynamic mechanical analyses (DMA 800, TA instruments) of the samples was conducted from room temperature to 200°C in the single cantilever mode at a heating rate and frequency of 3°C/min and 1 Hz, respectively. Thermogravimetric analysis (TGA) of the neat cured Epoxy and its composites with GnP was carried out using TGA 500 (TA instruments, USA) with a heating rate of 10°C /min from room temperature to 700°C in air. Flexural properties of the samples were tested using a United Testing System (UTS, SFM-20 load frame) with a 100 pound load cell according to the ASTM D790. The morphology of the fracture surface was observed by Scanning electron microscopy (Carl Zeiss Varible Pressure SEM EVO LS25). Samples were sputter-coated with tungsten prior to their SEM observation.

3. Proposed Mechanism

Sugar azide (SA), a highly reactive substance, forms nitrenes by thermal or photocatalytic decomposition. The in-situ formed nitrenes react with the double bonds at the edges of GnP to form the azide adduct. Finally, the -OAc groups were hydrolyzed to form hydroxyl terminated azide modified GnP (SAMG). The pathway of SAMG formation has been shown in Scheme 1.

4. Results and Discussion

4.1. Characterization of Functionalized Graphene (SAMG)

4.1.1. XPS

Fig. 1a and b show the C-1s XPS patterns of GnP and SAMG, respectively. The spectrum of GnP can be deconvoluted into two different peaks. The peaks at 284.8 and 289.3 eV have been assigned to the C–C/C=C in the aromatic rings, and O–C=O groups, respectively [13-15].

However, C-1s XPS patterns of SAMG have been deconvoluted into four different peaks. Appearance of two new peaks at 285.6 and 286.5eV has been assigned to C-N and C-OH groups, respectively. The N-1s spectrum of SAMG is shown in the inset of Fig. 1b. The well-defined peaks at 398.9 and 401.7 eV clearly suggest the existence of bonded nitrogen in SAMG.

4.1.2. AFM

AFM characterization allows identification of the number of graphene layers. AFM image of SAMG is shown in Fig. 2. The thickness of SAMG, measured from the height profile of the AFM image, is about 1.45 nm. The thickness of the SAMG sheets was drastically reduced compared to neat GnP (5-7nm) indicating successful exfoliation of graphene layers upon functionalization. However, the height value of SAMG compared to theoretical value of monolayer of graphene is due to i) the presence of the oxygenated moiety as a result of functionalization and ii) the resulting few layers (4-5) of graphene.

4.1.3. TGA

TGA thermograms of GnP and SAMG has been shown in Fig. 3 and the derivative plot (DTG) is shown in inset of Fig.3. Neat GnP is quite stable up to 450^{O}C. The weight loss after 450^{O}C is due to degradation of carbon skeleton of GnP. On the other hand, SAMG exhibited almost 5% weight loss at 400^{O}C. DTG curve showed that thermal history of SAMG is associated with two-step degradation process. Initial weight loss in the temperature range of 150-210 ^{O}C corresponds to the combined weight loss due to degradation of oxygenated groups and the azide which have been formed upon functionalization. The final weight loss at around 500 ^{O}C is due to cleavage of carbon skeleton of GnP.

4.1.4. Raman Spectroscopy

Raman spectroscopic analysis is an important tool to define the quality of graphene. Figs. 4a and 4b show the Raman spectra of GnP and SAMG, respectively. The Raman spectrum of GnP has the characteristic D band at 1352 cm^{-1} (the breathing mode of C-sp^2 atoms in the rings and is related to the disorder within the structure) and a G band at 1572 cm^{-1} (the in-plane bond stretching motion of C-sp^2 atoms) [16-19]. However, Raman spectrum of SAMG (Fig. 4b) showed an increment in I_D:I_G ratio from 0.54 to 0.77 attributed to the enhancement in defect

concentration due to functionalization, i.e., conversion of π-bonded C-sp^2 carbons to C-sp^3 ones. Moreover, the higher I_D/I_G ratio signifies a higher degree of covalent functionalization [20]. However, the shape of 'G' band at 1579 cm^{-1} was observed to be sharp suggesting that the functionalization occurred at the edges without disrupting the basal plane of GnP.

4.1.5. SEM

SEM micrographs of neat GnP and SAMG are shown in Figs. 5a and 5b. The surface of GnP was smooth and clean (Fig. 5a). However, extensive functionalization did not affect the basal plane or the flaky structure of GnP. but, the surface of SAMG became rough and wavy after functionalization (Fig. 5b).

4.2. Thermo-mechanical Performance of Epoxy/SAMG Composite

4.2.1. TGA

The thermal stability of neat Epoxy and its nanocomposites is shown in Fig. 6. Onset degradation temperature of neat Epoxy appeared at 355^OC. However, the onset degradation temperature was reduced to 339^OC for Epoxy/GnP nanocomposite. At 50% weight loss, the degradation temperatures of neat Epoxy, Epoxy/GnP, and Epoxy/SAMG nanocomposites were observed to be 394, 382, and 408^OC, respectively. The decrease in thermal stability of Epoxy/GnP nanocomposite was probably due to poor interfacial adhesion between filler and matrix resulting from inhomogeneous distribution of GnP particles throughout the matrix. On the other hand, functionalization resulted in the creation of polar groups which in turn facilitate homogeneous distribution of SAMGs throughout the matrix. Homogeneously distributed functionalized graphene layers could reduce the emission of small gaseous molecules resulting in delayed thermal degradation of the nanocomposites compared to neat Epoxy and Epoxy/GnP composite.

4.2.2. DMA

The variation of loss tangent (Tanδ) as a function of temperature is shown in Fig. 7. Tanδ is the ratio of the loss modulus to the storage modulus and is very sensitive to structural transformations. Tanδ for neat Epoxy appears at 153.7^OC, which is assumed to be the glass transition temperature (Tg) of the neat Epoxy. However, in presence of GnP, Tg has shifted to lower temperature region (144.8^OC) suggesting partial immiscibility between the matrix and

filler, leading to the poor interfacial adhesion. However, functionalization resulted in a substantial increment in Tg suggesting the formation of better adhesion and a strong interface between SAMG and Epoxy. Superior adhesion allows better stress transfer from filler to matrix. The details of thermal stability and Tg's of neat Epoxy and nanocomposites have been summarized in Table 1.

4.2.3. SEM

Fractured surfaces (from flexural tests) of neat epoxy and epoxy nanocomposites were investigated by SEM and the micrographs are presented in in Figs. 8 (a-d). The fracture surfaces of neat Epoxy were smooth and clean (Fig. 8a). Epoxy/GnP nanocomposite displayed the clear formation GnP aggregates. The aggregates were very poorly distributed in the matrix which was responsible for its poor thermal and mechanical properties (Fig. 8b). On the other hand, functionalization caused a more homogeneous distribution of SAMGs throughout the matrix (Fig. 8c); High magnification SEM image of Epoxy/SAMG nanocomposite (Fig. 8d) further showed that the wavy SAMG particles were embedded into the matrix suggesting better wetting and stronger bonding between Epoxy and SAMG which in turn caused an improvement in thermal and mechanical properties to a reasonable extent.

4.2.4. Flexural Properties

Fig. 9 represents the effect of functionalization on the flexural modulus and strength of GnP/epoxy nanocomposites. Functionalization resulted in an 18% improvement in flexural modulus as compared to neat epoxy. Functionalization of GnP results in: (a) Creation of groups which can react with Epoxy matrix and (b) prevention of restacking of GnP nanoparticles which helps produce a more homogeneous distribution. The flexural strength of Epoxy/SAMG nanocomposite system showed a negligible increment.

5. Conclusions

Nitrogen-linked graphene was synthesized using sugar azide via the formation of nitrene as an intermediate. Polar groups created via functionalization facilitated hybrid nanocomposite formation with improved thermo-mechanical properties. Functionalization of graphene has been verified with spectroscopic studies and thermal analysis. The nanocomposite showed a

reasonable increase in glass transition temperature as compared to neat matrix and the Epoxy/GnP composite suggesting strong interfacial adhesion between functionalized graphene and the Epoxy. Morphological observation revealed that the Functionalized GnPs were rough, wavy and were embedded into the matrix confirming the strong adhesion between filler and matrix. The flexural modulus was 18% higher compared to neat Epoxy.

Acknowledgement

This material is based upon work supported by the United States Army under Contract No. W56HZV-13-C-0401. The authors are thankful to XG Sciences, Inc. for supplying the graphene nanoplatelets.

References

1. Fan X, Peng W, Li Y, Li X, Wang S, Zhang G, Zhang F. Deoxygenation of Exfoliated Graphite Oxide under Alkaline Conditions: A Green Route to Graphene Preparation. Adv Mater, **20,** 4490(2008). DOI: 10.1002/adma.200801306
2. Geim AK, Novoselov KS. The rise of graphene. Nat Mater, **6**, 183 (2007). DOI:10.1038/nmat1849
3. Wang G, Yang J, Park J, Gou X, Wang B, Liu H, Yao J. Facile Synthesis and Characterization of Graphene Nanosheets. J Phys Chem C, **112**, 8192 (2008). DOI: 10.1021/jp710931h
4. Lee C, Wei X, Kysar JW, Hone J. Measurement of the Elastic Properties and Intrinsic Strength of Monolayer Graphene. Science, **321**, 385 (2008). DOI: 10.1126/science.1157996
5. Chen H, Muller MB, Gilmore KJ, Wallace GG, Li D. Mechanically Strong, Electrically Conductive, and Biocompatible Graphene Paper. Adv Mater, **20**, 3557 (2008). DOI: 10.1002/adma.200800757
6. Stankovich S, Dikin DA, Dommett GHB, Kohlhaas KM, Zimney EJ, Stach EA, Piner RD, Nguyen ST, Ruoff RS. Graphene-based composite materials. Nature, **442**, 282 (2006). DOI:10.1038/nature04969

7. Balandin AA, Ghosh S, Bao W, Calizo I, Teweldebrhan D, Miao F, Lau CN. Superior Thermal Conductivity of Single-Layer Graphene. Nano Lett, **8**, 902(2008). DOI: 10.1021/nl0731872
8. Navarro CG, Weitz RT, Bittner AM, Scolari M, Mews A, Burghard M, Kern K. Electronic Transport Properties of Individual Chemically Reduced Graphene Oxide Sheets. Nano Lett, **7**, 3499 (2007). DOI: 10.1021/nl072090c
9. Zhang Y, Tang TT, Girit C, Hao Z, Martin MC, Zettl A, Crommie MF, Shen YR, Wang F. Direct observation of a widely tunable bandgap in bilayer graphene. Nature, **459**, 820 (2009). DOI:10.1038/nature08105
10. Li D, Muller MB, Gilje S, Kaner RB, Wallace CG. Processable aqueous dispersions of graphene nanosheets. Nature Nanotechnol, **3**, 101(2008). DOI:10.1038/nnano.2007.451
11. Si Y, Samulski ET. Synthesis of Water Soluble Graphene. Nano Lett, **8**, 1679(2008). DOI: 10.1021/nl080604h
12. Bai H, Xu Y, Zhao L, Li C, Shi G. Non-covalent functionalization of graphene sheets by sulfonated polyaniline. Chem Commun, **13**, 1667(2009). DOI: 10.1039/B821805F
13. Bose S, Kuila T, Mishra A, Kim NH, Lee JH. Dual role of glycine as a chemical functionalizer and a reducing agent in the preparation of graphene: an environmentally friendly method. J Mater Chem, **22**, 9696(2012). DOI: 10.1039/C2JM00011C
14. Zhou X, Zhang J, Wu H, Yang H, Zhang J, Guo S. Reducing Graphene Oxide via Hydroxylamine: A Simple and Efficient Route to Graphene. J Phys Chem C, **115**, 11957(2011). DOI: 10.1021/jp202575j
15. Lin Z, Yao Y, Li Z, Liu Y, Li Z, Wong CP. Solvent-Assisted Thermal Reduction of Graphite Oxide. J Phys Chem C, **114**, 14819(2010). DOI: 10.1021/jp1049843
16. Kudin KN, Ozbas B, Schniepp HC, Prud'homme RK, Aksay IA, Car R. Raman Spectra of Graphite Oxide and Functionalized Graphene Sheets. Nano Lett, **8**, 36(2008). DOI: 10.1021/nl071822y
17. Cancado LG, Pimenta MA, Neves BRA, Dantas MSS, Jorio A. Influence of the Atomic Structure on the Raman Spectra of Graphite Edges. Phys Rev Lett, **93**, 247401(2004). DOI: http://dx.doi.org/10.1103/PhysRevLett.93.247401

18. Ferrari AC. Raman spectroscopy of graphene and graphite: Disorder, electron–phonon coupling, doping and nonadiabatic effects. Solid State Commun, **143**, 47(2007). DOI: 10.1016/j.ssc.2007.03.052
19. Bose S, Kim NH, Kuila T, Lau AKT, Lee JH. Electrochemical performance of a graphene/polypyrrole nanocomposite as a supercapacitor electrode. Nanotechnology, **22**, 295202(2011). doi:10.1088/0957-4484/22/29/295202
20. Leinonen H, Pettersson M, Lajunen M, Water-soluble carbon nanotubes through sugar azide functionalization. Carbon, **49**, 1299(2011). DOI: 10.1016/j.carbon.2010.11.049

Figure captions:

Fig. 1: XPS of (a) neat GnP and (b) SAMG.

Fig. 2: Non-contact mode AFM image of SAMG on mica substrate.

Fig. 3: TGA thermograms of GnP and SAMG. The derivative curve is shown in inset.

Fig. 4: Raman spectroscopy of (a) neat GnP and (b) SAMG.

Fig. 5: High magnification SEM image of (a) neat GnP and (b) SAMG.

Fig. 6: TGA thermograms of neat Epoxy and Epoxy/GnP nanocomposites. The zoomed in image of onset degradation is shown in inset.

Fig. 7: Variation of glass transition temperature as a function of temperature of neat Epoxy and Epoxy/GnP nanocomposites.

Fig. 8: SEM image (flexural fractured) of (a) neat GnP; (b) Epoxy/GnP nanocomposite; Epoxy/SAMG nanocomposite at (c) lower and (d) higher magnification.

Fig. 9: Flexural properties of neat Epoxy and Epoxy/GnP nanocomposites.

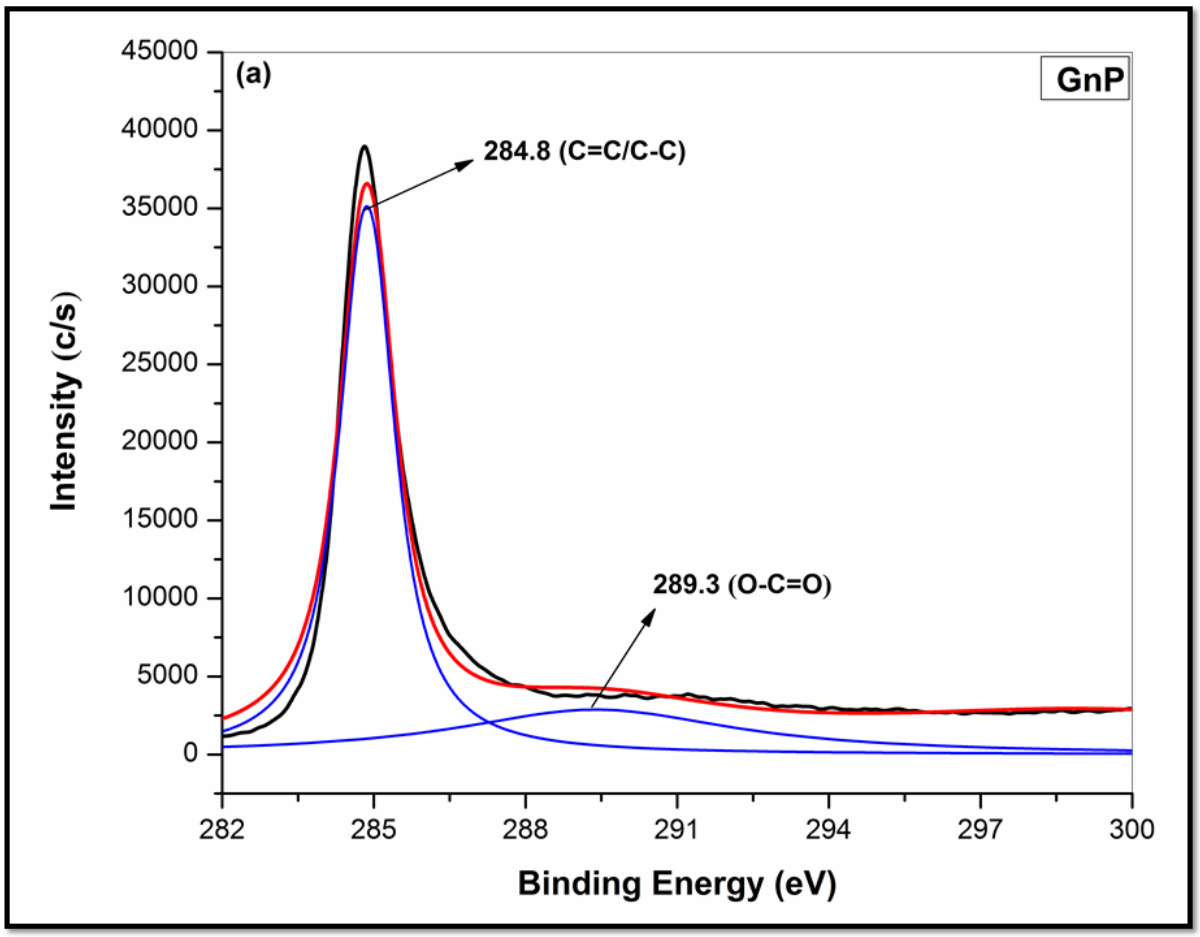
(a)
GnP
284.8 (C=C/C-C)
289.3 (O-C=O)
Intensity (c/s)
Binding Energy (eV)
45000
40000
35000
30000
25000
20000
15000
10000
5000
0
282
285
288
291
294
297
300

Fig. 1a

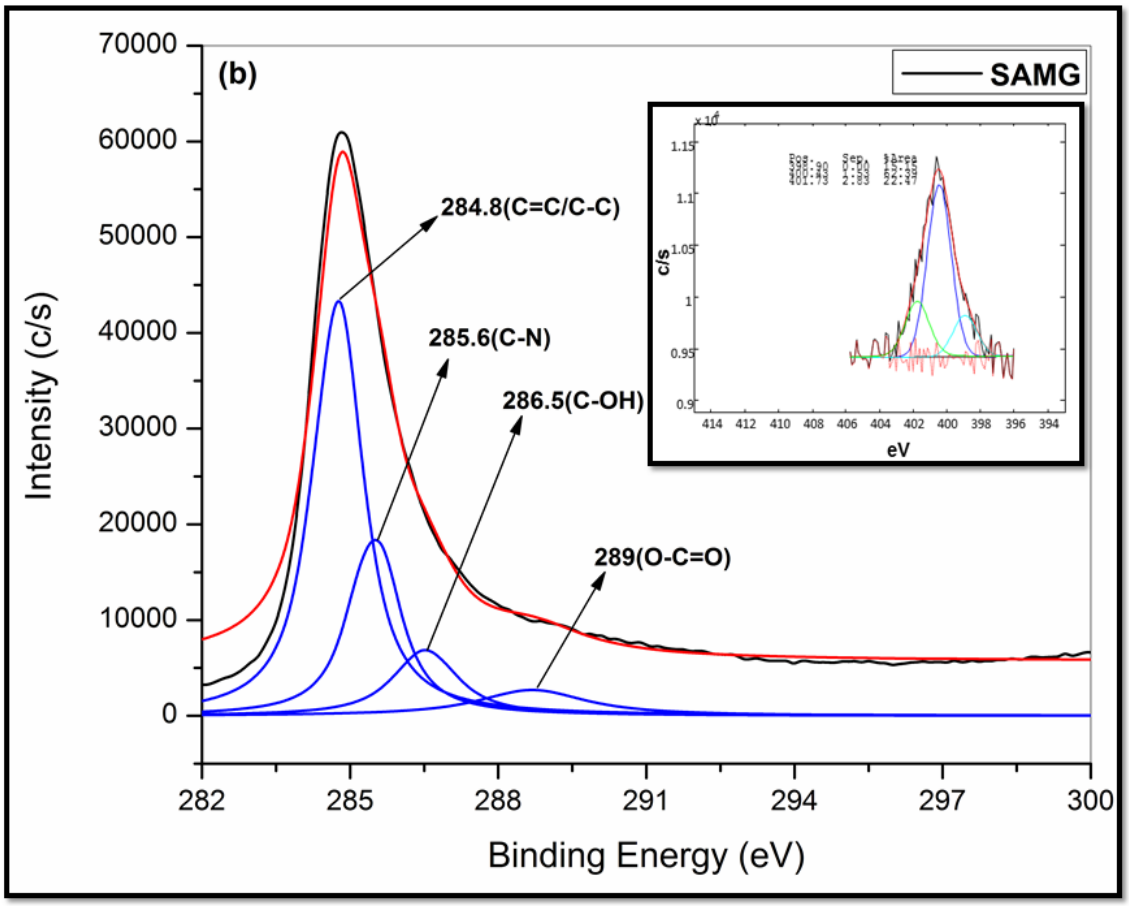
(b)
SAMG
284.8(C=C/C-C)
285.6(C-N)
286.5(C-OH)
289(O-C=O)
Intensity (c/s)
Binding Energy (eV)
70000
60000
50000
40000
30000
20000
10000
0
282
285
288
291
294
297
300
c/s
eV
414
412
410
408
406
404
402
400
398
396
394

Fig. 1b

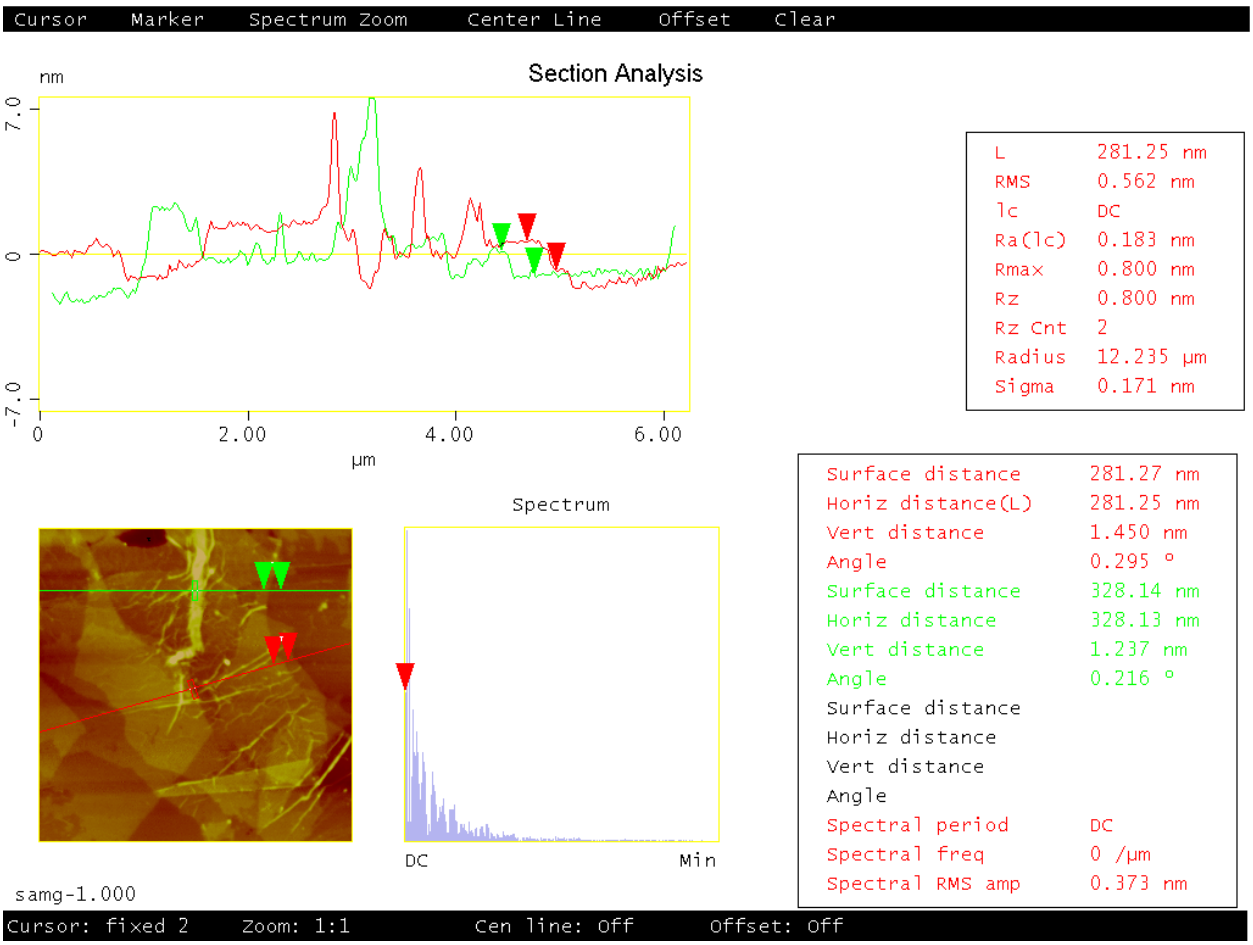
Cursor Marker Spectrum Zoom Center Line Offset Clear
Section Analysis
nm
7.0
0
-7.0
0
2.00
4.00
6.00
µm
L 281.25 nm
RMS 0.562 nm
lc DC
Ra(lc) 0.183 nm
Rmax 0.800 nm
Rz 0.800 nm
Rz Cnt 2
Radius 12.235 µm
Sigma 0.171 nm
Spectrum
DC
Min
Surface distance 281.27 nm
Horiz distance(L) 281.25 nm
Vert distance 1.450 nm
Angle 0.295 °
Surface distance 328.14 nm
Horiz distance 328.13 nm
Vert distance 1.237 nm
Angle 0.216 °
Surface distance
Horiz distance
Vert distance
Angle
Spectral period DC
Spectral freq 0 /µm
Spectral RMS amp 0.373 nm
samg-1.000
Cursor: fixed 2 Zoom: 1:1 Cen line: Off Offset: Off

Fig. 2

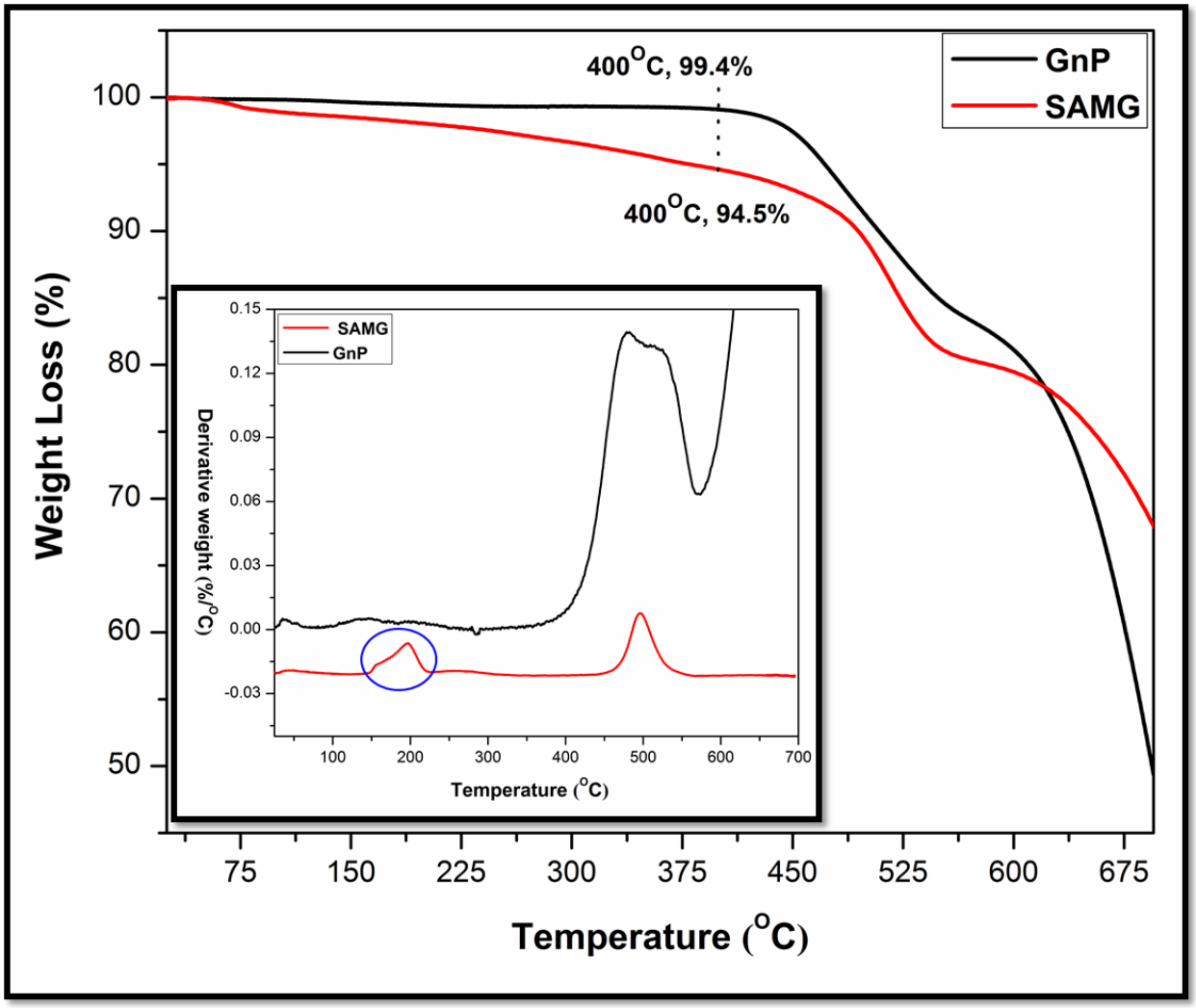
400°C, 99.4%
400°C, 94.5%
GnP
SAMG
Weight Loss (%)
Temperature (°C)
Derivative weight (%/°C)
SAMG
GnP
Temperature (°C)

Fig. 3

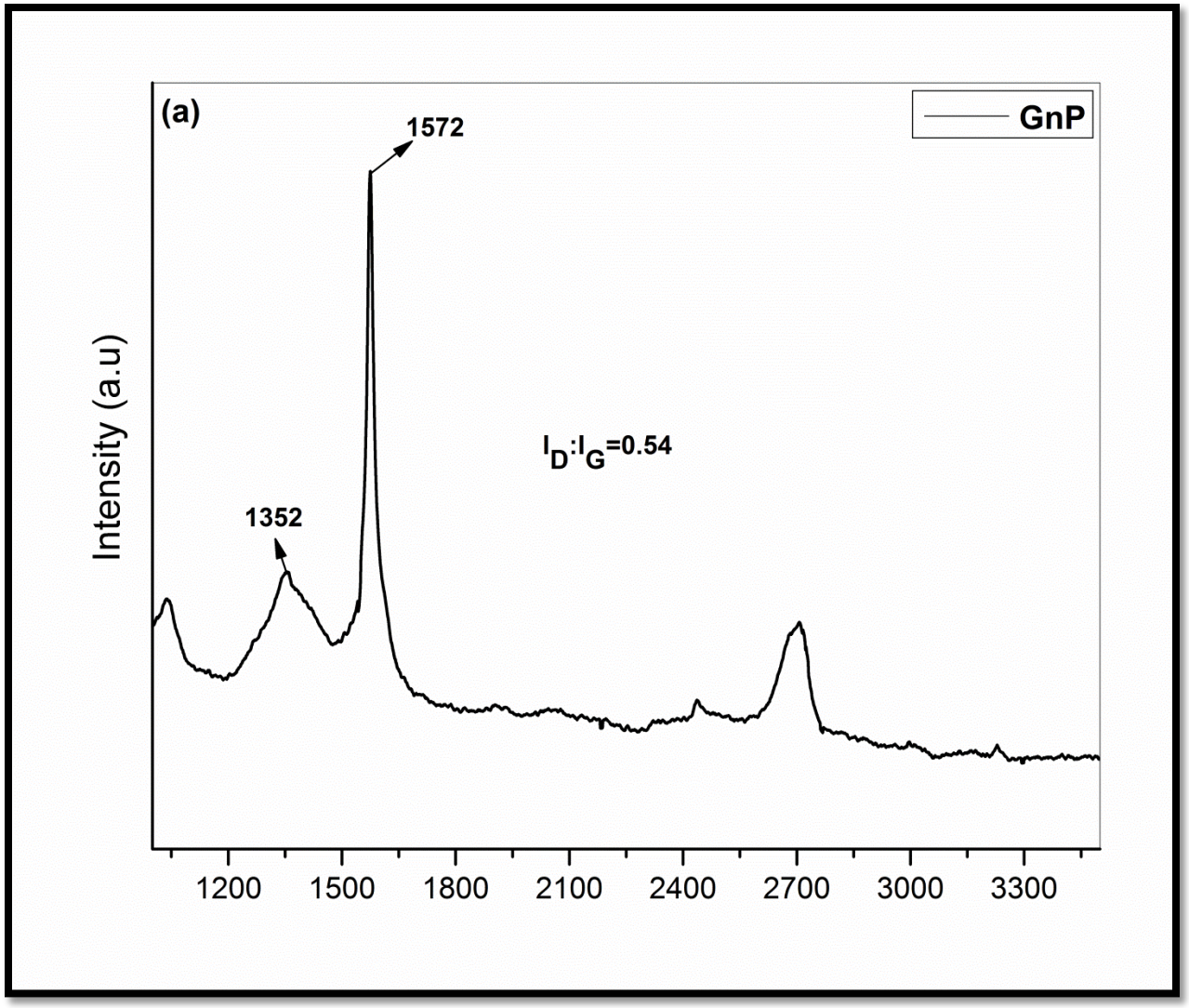
(a)
GnP
1572
1352
$I_D:I_G$=0.54
Intensity (a.u)
1200
1500
1800
2100
2400
2700
3000
3300

Fig. 4a

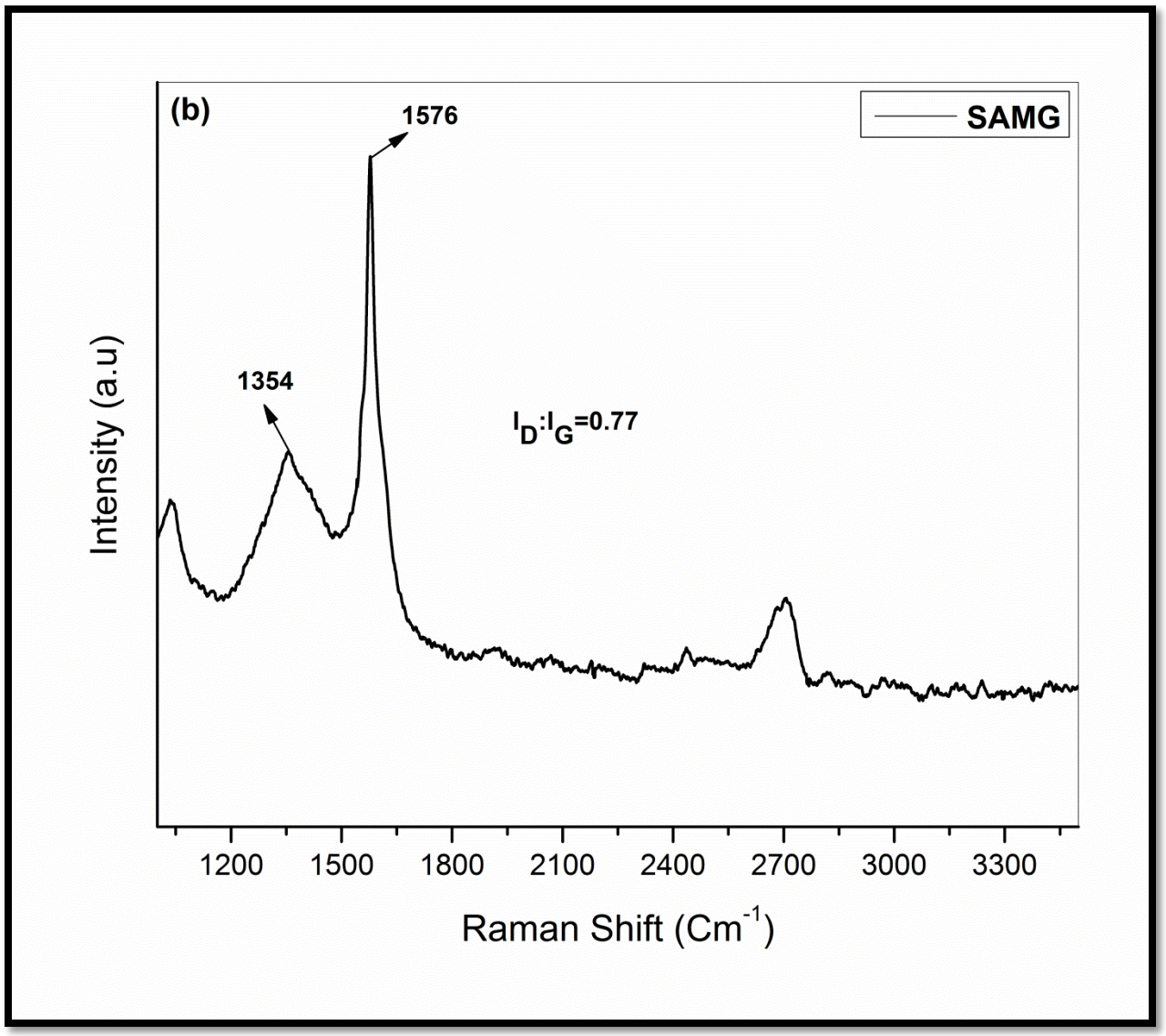
(b)
1576
SAMG
1354
$I_D:I_G$=0.77
Intensity (a.u)
1200
1500
1800
2100
2400
2700
3000
3300
Raman Shift (Cm^{-1})

Fig. 4b

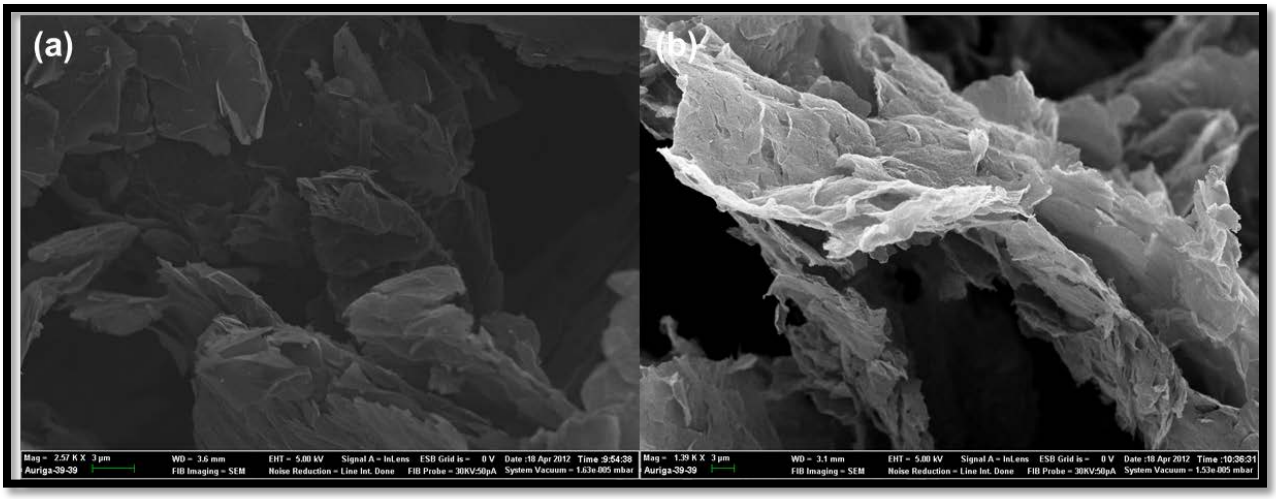

Fig. 5

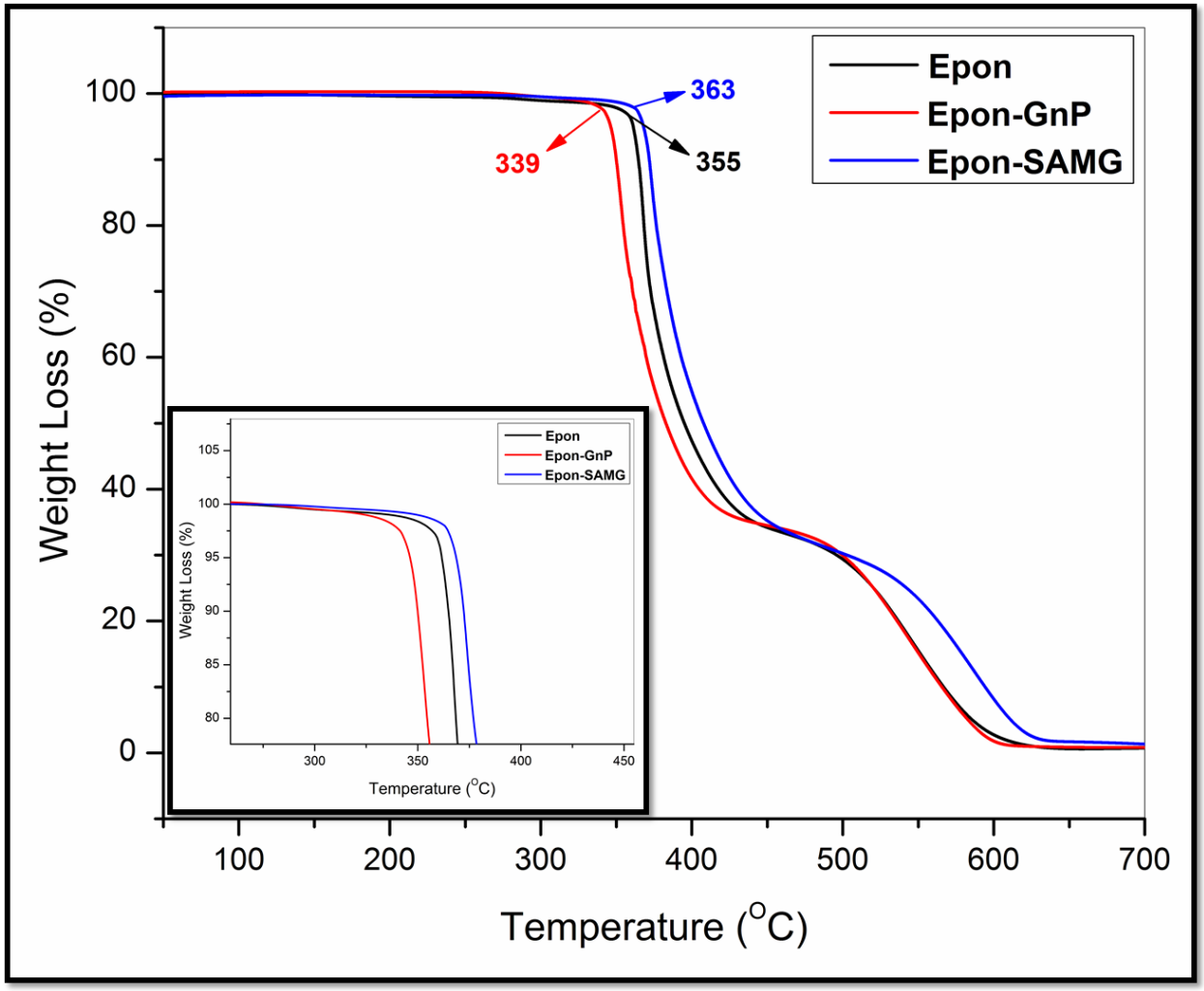
Epon
Epon-GnP
Epon-SAMG
363
339
355
Weight Loss (%)
Temperature (°C)
100
80
60
40
20
0
100
200
300
400
500
600
700
105
95
90
85
80
300
350
400
450

Fig. 6

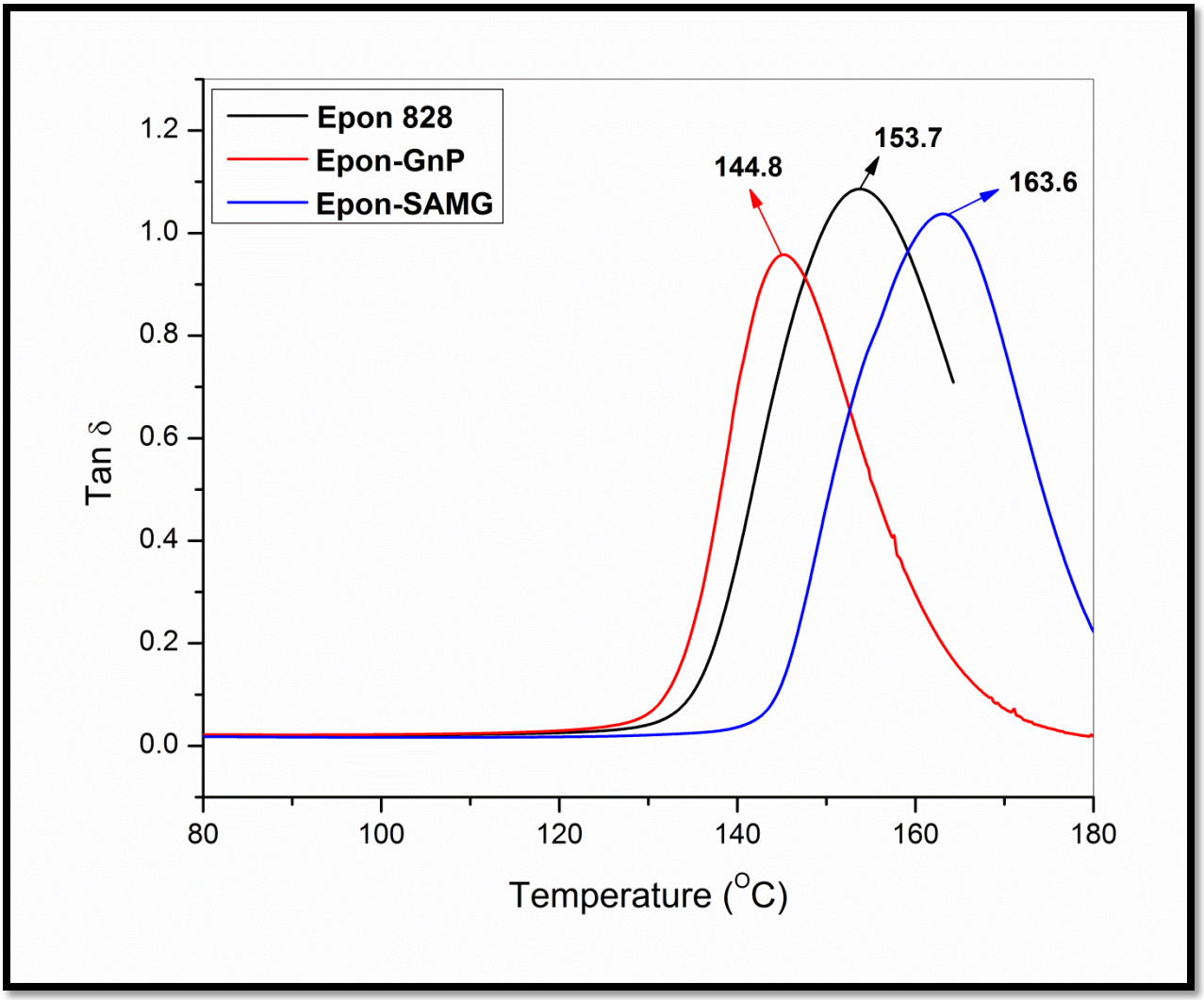
Epon 828
Epon-GnP
Epon-SAMG
144.8
153.7
163.6
Tan δ
1.2
1.0
0.8
0.6
0.4
0.2
0.0
80
100
120
140
160
180
Temperature (°C)

Fig. 7

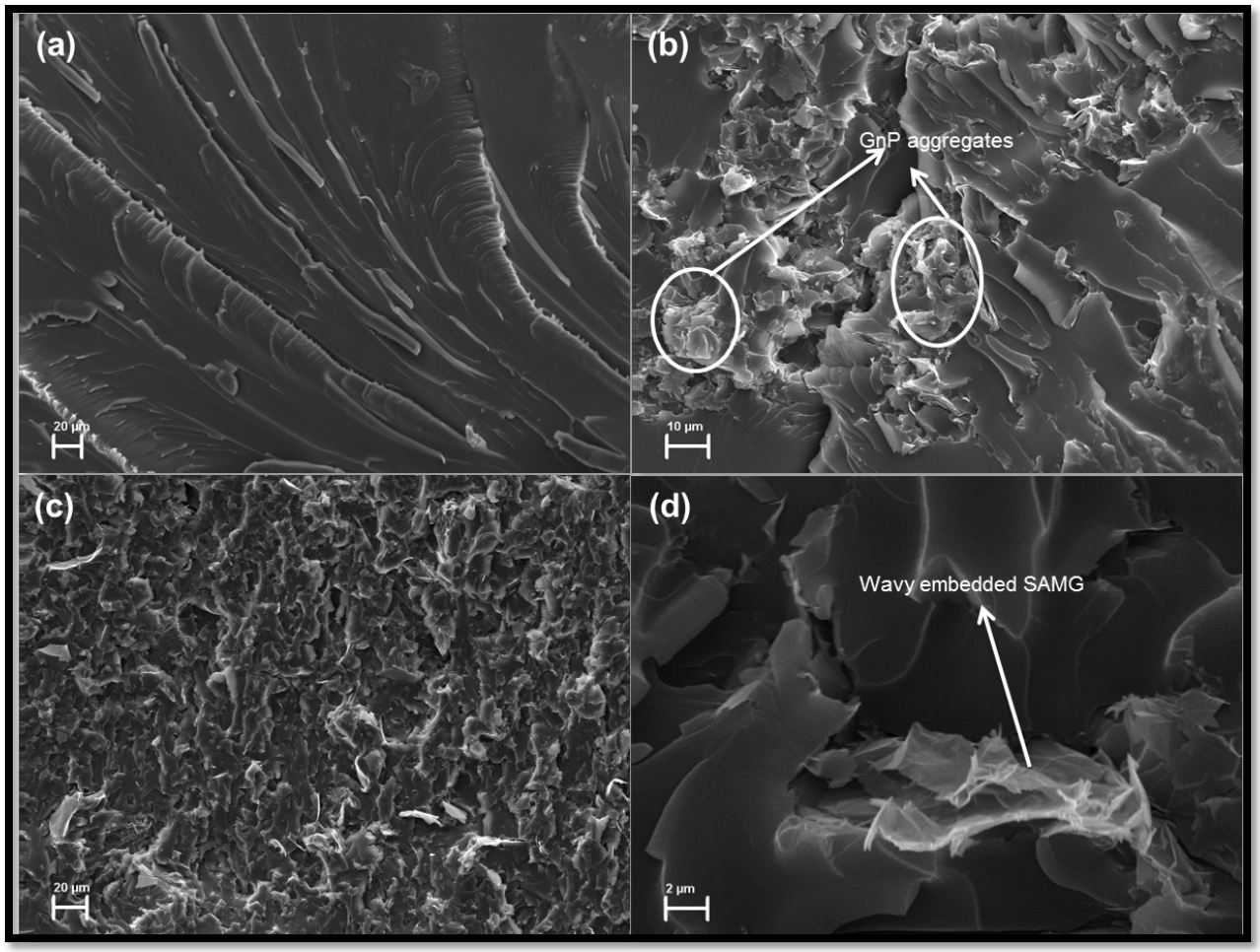

Fig. 8

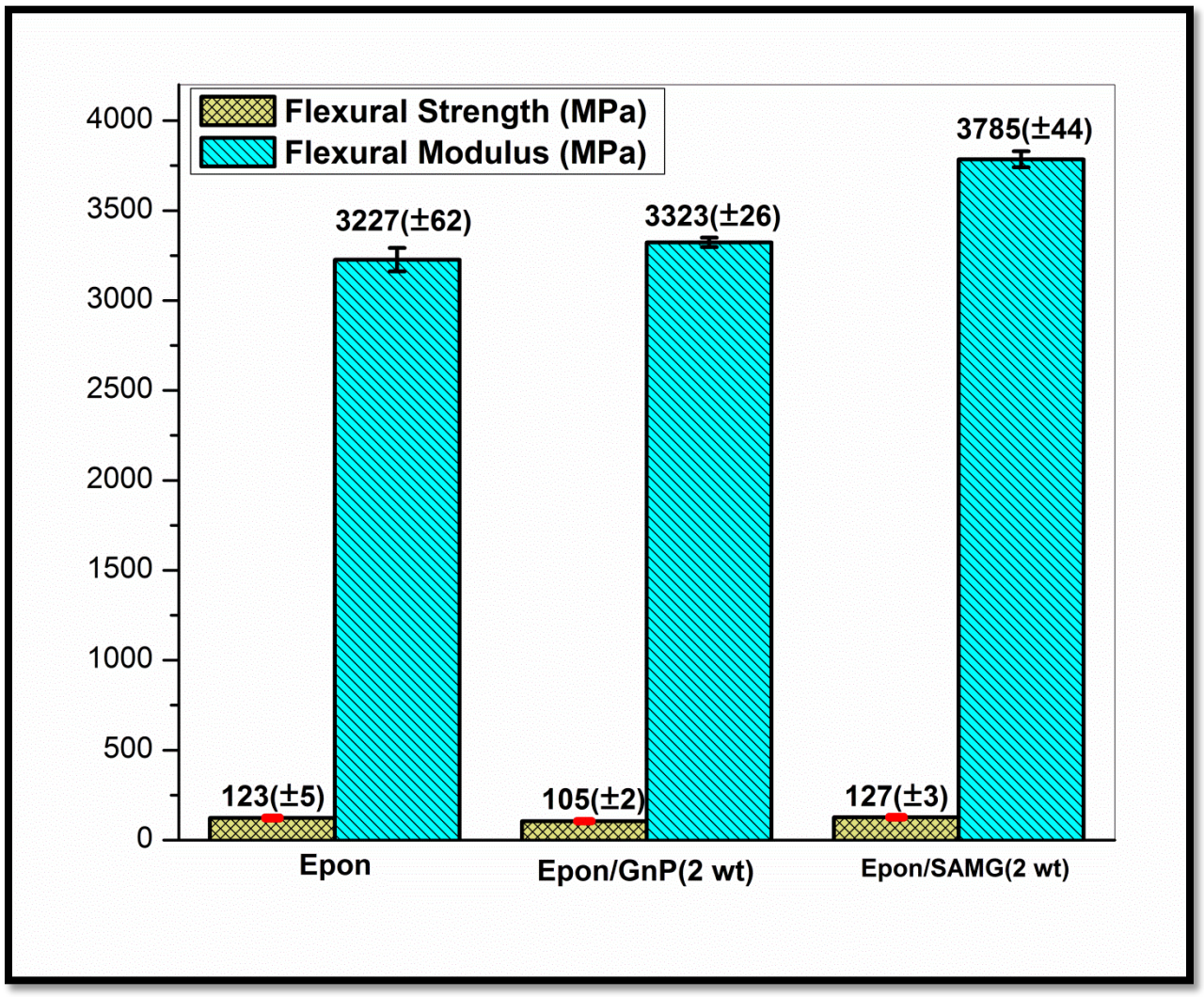
Flexural Strength (MPa)
Flexural Modulus (MPa)
4000
3500
3000
2500
2000
1500
1000
500
0
3227(±62)
3323(±26)
3785(±44)
123(±5)
105(±2)
127(±3)
Epon
Epon/GnP(2 wt)
Epon/SAMG(2 wt)

Fig. 9

Table 1: Thermal stability and dynamic mechanical properties of neat Epoxy and its nanocomposites with GnP

Sample	Onset degradation temperature (^{O}C)	Degradation temperature at 50% weight loss (^{O}C)	Glass transition temperature (^{O}C)	Tanδ_{max}
Neat Epon	355	394	153.7	1.09
Epon/GnP (2%)	339	384	144.8	0.95
Epon/SAMG (2%)	363	408	163.6	1.03